

Electron Paramagnetic Resonance of Fe^{3+} and Ni^{3+} in KTaO_3 †

D. M. HANNON*

Gordon McKay Laboratory, Harvard University, Cambridge, Massachusetts

(Received 28 July 1967)

The electron paramagnetic resonance of Fe^{3+} and Ni^{3+} in KTaO_3 is reported. Both impurity ions are substitutional at the two cation sites of the host. For Fe^{3+} the room-temperature a values are $288 \pm 5 \times 10^{-4} \text{ cm}^{-1}$ for Fe^{3+} on the Ta^{5+} site, and $30 \pm 1 \times 10^{-4} \text{ cm}^{-1}$ for Fe^{3+} on the K^{+1} site. The temperature variation of these parameters is discussed. Ni^{3+} at the Ta^{5+} is in a low-spin configuration and undergoes a Jahn-Teller axial distortion. Estimates of $10Dq$ from g -shift formulas and axial ground-state splitting from line broadening are given. The resonance of Ni^{3+} at the K^{+1} site indicates a negative crystal field with a $10Dq$ value of 7400 cm^{-1} derived from a g -shift formula.

I. INTRODUCTION

THIS paper reports the electron paramagnetic resonance (EPR) of Fe^{3+} and Ni^{3+} in the perovskite crystal KTaO_3 . Although KTaO_3 was chosen because of its close relation to ferroelectric materials, the results discussed here are of interest more for their contribution to EPR and related crystal field studies than for their ability to illuminate the dielectric properties of the host. A future paper will discuss the EPR spectra of Mn^{4+} in KTaO_3 where anomalous temperature effects are manifested which may be related to the "soft" ferroelectric mode of the host.

KTaO_3 has a perovskite structure isomorphous with the cubic phase of the familiar BaTiO_3 . Early reports listed KTaO_3 as a ferroelectric with a Curie temperature near 13°K .^{1,2} However, an investigation by Wemple³ showed that KTaO_3 remains in a cubic, nonpolar state down to 4.2°K and does not undergo a phase transition to a ferroelectric state. The variations of Curie temperature in earlier measurements have been attributed to impurities of sodium or fluorine in the KTaO_3 crystal.³

The most interesting result reported is that both magnetic impurities, Fe^{3+} and Ni^{3+} , are substitutional at both cation sites. In most of the samples measured the trivalent ion group impurities dutifully follow ionic size considerations and occupy the Ta^{5+} site, but occasionally these ions show up at or near the much larger K^{+1} site. The crystal field at this site is quite different from the field at the Ta^{5+} site and this difference is clearly indicated by the qualitatively different EPR results.

The resonances were observed over a temperature range of 4.2°K to room temperature and above. Wemple³ has previously reported the EPR of Fe^{3+} in KTaO_3 at helium temperature, and our results agree, with some minor exceptions, with his work.

* Supported by U.S. Air Force Cambridge Research Laboratory AF 19-(628)-3874.

† Present address: IBM Research Laboratory, San Jose, California.

¹ B. T. Matthias, Phys. Rev. **75**, 1771 (1949).

² J. K. Hulm, B. T. Matthias, and F. A. Long, Phys. Rev. **79**, 885 (1949).

³ S. H. Wemple, Ph.D. thesis, Massachusetts Institute of Technology, Cambridge, Massachusetts, 1963 (unpublished).

II. CRYSTAL GROWING TECHNIQUE

The complete phase diagram for the system K_2CO_3 - Ta_2O_5 is given by Reisman *et al.*⁴ The desired phase is $\text{K}_2\text{O-Ta}_2\text{O}_5$ which occurs, of course, for 1:1 mole ratio of K_2CO_3 and Ta_2O_5 with CO_2 being given off during heating. Since K_2CO_3 is more volatile than Ta_2O_5 we begin with an excess of K_2CO_3 . Our simple recipe is the following: a platinum crucible charged with 20 g of Ta_2O_5 and 9.2 g of K_2CO_3 is held at 1450°C for 1-2h. The temperature is then lowered at 20°C per hour. These directions are not critical and substantial deviations from them may still produce crystals. The crystals average about $\frac{1}{2} \text{ cm}$ on a side; occasionally much larger crystals appear.

Crystals grown in the above manner are deep blue and have high conductivity, both effects being caused by free carriers which absorb in the red. These carriers are present because oxygen vacancies reduce the tantalum to Ta^{4+} or Ta^{3+} , which in turn act to provide donor levels lying near the conduction band.³ To eliminate these free carriers, we add a moderate amount of TiO_2 , $\sim \frac{1}{2} \text{ g}$, to the recipe. The titanium, Ti^{4+} , substitutes for Ta^{5+} and recovers the charge balance in the presence of oxygen vacancies thus eliminating most of the reduced tantalum. Wemple³ and Bonner *et al.*⁵ add SnO_2 to provide this type of compensation.

The single crystal $\text{K}_{1-x}\text{Na}_x\text{TaO}_3$, with x approximately 0.3, was also studied. Figure 1 shows the dielectric constant versus temperature for the crystals KTaO_3 and $\text{K}_{0.7}\text{Na}_{0.3}\text{TaO}_3$. It should be mentioned that both samples also contained magnetic impurity ions. The KTaO_3 dielectric constant follows a Curie-Weiss law down to approximately 60°K ; below this temperature the dielectric constant falls below the predicted Curie-Weiss law and remains in the nonpolar state at all temperatures. The crystal $\text{K}_{0.7}\text{Na}_{0.3}\text{TaO}_3$ has a dielectric constant which follows a Curie-Weiss law quite closely and goes through a second order ferroelectric phase transition at 48°K . Davis⁶ has studied the system $\text{K}_{1-x}\text{Na}_x\text{TaO}_3$ for $0 < x < 1$ and

⁴ A. Reisman, F. Holtzberg, M. Berkenblit, and M. Berry, J. Am. Chem. Soc. **78**, 4514 (1956).

⁵ W. A. Bonner, E. F. Dearborn, and L. G. Van Uitert, Am. Ceram. Soc. Bull. **44**, 9 (1965).

⁶ T. G. Davis, thesis, Massachusetts Institute of Technology, Cambridge, Massachusetts, 1965 (unpublished).

reports that the ferroelectric transition temperature increases with increasing x to a maximum of 65°K at $x=0.5$. A further increase of x causes the transition temperature to decrease to $\sim 0^\circ\text{K}$ at $x=0.7$.

The failure of KTaO_3 to become ferroelectric is characteristic of crystals with low Curie temperatures. Such crystals, which might be termed incipient ferroelectrics, have their predicted transition temperatures too low for the usual high-temperature approximations, which lead to a Curie-Weiss law, to hold.⁷ For example, Cochran⁸ invokes anharmonicity of the lattice to arrive at the Curie-Weiss relation, an obvious high-temperature approximation. Other crystals showing this dielectric behavior are SrTiO_3 ,⁹ Pb-doped $\text{Cd}_2\text{Nb}_2\text{O}_7$,¹⁰ LiTl tartrate,¹¹ and SnTe .¹²

III. EXPERIMENTAL RESULTS

A. Impurity Sites

Before describing the EPR results, we first consider the possible sites for impurity ions in the KTaO_3

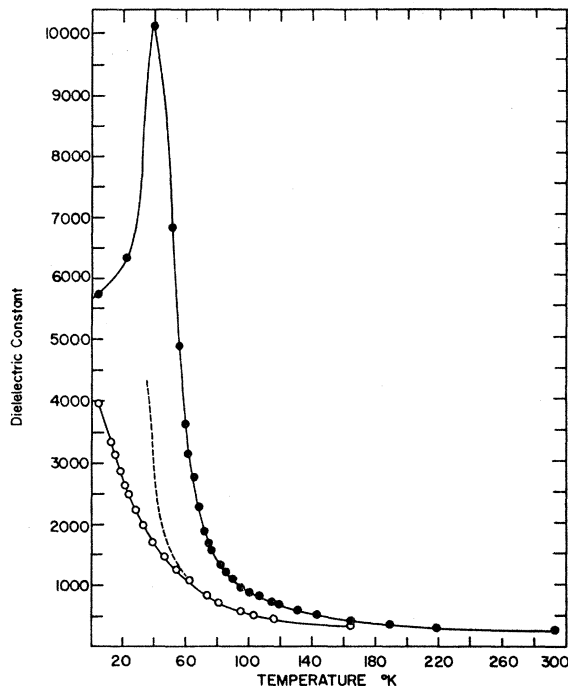


FIG. 1. Dielectric constant of KTaO_3 and $\text{K}_{0.7}\text{Na}_{0.3}\text{TaO}_3$ versus temperature. Open circles are points for KTaO_3 and fit a relation $\epsilon = 60 + (3.3 \times 10^4)/(T - 27^\circ\text{K})$ above 60°K . The dashes indicate a continuation of this curve below 60°K . The closed circles are points for $\text{K}_{0.7}\text{Na}_{0.3}\text{TaO}_3$ and fit the relation

$$\epsilon = 49 + (4.3 \times 10^4)/(T - 48^\circ\text{K})$$

Note that the crystals contain magnetic impurities which can affect the dielectric constant.

⁷ J. H. Barrett, *Phys. Rev.* **86**, 118 (1952).

⁸ W. Cochran, *Advan. Phys.* **9**, 387 (1960).

⁹ J. K. Hulm, *Proc. Phys. Soc. (London)* **A63**, 1184 (1950).

¹⁰ J. K. Hulm, *Phys. Rev.* **92**, 504 (1953).

¹¹ B. T. Matthias and J. K. Hulm, *Phys. Rev.* **82**, 108 (1951).

¹² G. S. Pawley, W. Cochran, R. A. Cowley, and G. Dolling, *Phys. Rev. Letters* **17**, 753 (1966).

perovskite structure. Fortunately, this impurity site determination is relatively easy. The close packing of the large K^{+1} and O^{-2} ions precludes interstices large enough to accommodate an impurity ion and the impurity must be substitutional at or quite close to one of the cation sites. For these cubic sites, and considering d electrons, only the fourth order term in a crystal-field expansion is operative in the spin resonance.

It is instructive to write this fourth order term V_4 for a point charge model for these two sites. At the Ta^{5+} site only the nearest neighbor oxygen ions need to be considered and we have

$$V_4(\text{Ta}^{5+}) = \frac{\frac{2}{3}(\sqrt{7}\pi)}{(d/2)^5} r^4 [(\sqrt{7})Z_{40} + (\sqrt{5})Z_{44}^c]. \quad (1)$$

However, at the K^{+1} site both nearest-neighbor oxygen and next-nearest-neighbor tantalum ions must be considered and we have

$$V_4(\text{K}^{+1}) = -\frac{\frac{1}{3}(\sqrt{7}\pi)}{(d/\sqrt{2})^5} r^4 [(\sqrt{7})Z_{40} + (\sqrt{5})Z_{44}^c] + \frac{(40/27)(\sqrt{7}\pi)}{[\frac{1}{2}(\sqrt{3})d]^6} r^4 [(\sqrt{7})Z_{40} + (\sqrt{5})Z_{44}^c], \quad (2)$$

where d is the unit cell dimension and r the distance from the site. The spherical harmonics are defined by Griffith.¹³ Equations (1) and (2) indicate the sharp difference in V_4 at the two sites. At the tantalum site V_4 is large and positive due to the close octahedrally coordinated oxygens. In contrast, V_4 at the potassium site is small and of uncertain sign. The first term in $V_4(\text{K}^{+1})$ is the contribution of the dodecahedrally arranged oxygens which is negative. The second term is the contribution of the eight Ta^{5+} ions which is close in magnitude and of opposite sign to the oxygen contribution. In fact, for a point-charge model the second term coming from the next nearest neighbors is larger than the first term from the oxygens. This weak crystal field at the dodecahedral A site in the ABO_3 perovskite structure has been discussed by various authors.^{14,15}

B. Ferric Ion, Fe^{3+}

1. Fe^{3+} in $(\text{K}, \text{Na})\text{TaO}_3$

In all cases investigated Fe^{3+} in a mixed crystal $(\text{K}, \text{Na})\text{TaO}_3$ showed only the $\frac{1}{2} \rightarrow -\frac{1}{2}$ transition¹⁶ together with lines reflecting strong axial fields. The fine structure lines are apparently inhomogeneously broadened by crystal-field variations due to random occupa-

¹³ J. S. Griffith, *The Theory of Transition Metal Ions* (Cambridge University Press, New York, 1961), p. 204.

¹⁴ L. Rimai and G. Demars, in *Paramagnetic Resonance*, edited by W. Low (Academic Press Inc., New York, 1963), p. 51.

¹⁵ R. S. Rubins and W. Low, in Ref. 14, p. 59.

¹⁶ W. Low, *Paramagnetic Resonance in Solids* (Academic Press Inc., New York, 1960).



FIG. 2. The hyperfine structure on the $\frac{1}{2} \rightarrow -\frac{1}{2}$ transition of Fe^{3+} in KTaO_3 caused by the nuclear spins of the K^{+1} ions.

tion of the A site by K^{+1} or Na^{+1} ions. Thus, we were unable to monitor the ferroelectric phase transition of $(\text{K}, \text{Na}) \text{TaO}_3$ crystals using EPR techniques as done in the system $\text{Fe}^{3+}:\text{BaTiO}_3$.¹⁷

2. Fe^{3+} on the Ta^{5+} Site in KTaO_3

Wemple³ measured the EPR of Fe^{3+} substituted on the Ta^{5+} site in KTaO_3 at helium temperature and reported a cubic field constant of $a = 345 \times 10^{-4} \text{ cm}^{-1}$ and a linewidth of 60 G. This compares to $a \approx 200 \times 10^{-4} \text{ cm}^{-1}$ and a linewidth of 8 G for Fe^{3+} in SrTiO_3 .¹⁸ As explained by Wemple,³ the interesting cause of the linewidth of Fe^{3+} is superhyperfine interaction between the ferric ion on the tantalum site and the nuclei ($I = \frac{3}{2}$) of the next-nearest-neighbor potassium ions. For lightly doped $\text{Fe}^{3+}:\text{KTaO}_3$ crystals this hyperfine splitting can be resolved as shown in Fig. 2. The hyperfine structure of Fig. 2 is seen only for H_{dc} along a $[100]$ axis and a rotation of $\sim 10^\circ$ from this direction will wash out the structure. In a $[100]$ direction the eight neighboring K^{+1} nuclei are equivalent yielding a total nuclear moment of $I_t = 12$ and $2I_t + 1 = 25$ hyperfine lines. Figure 2 shows a spectrum approaching that number. The resolved linewidth is 3 G and the hyperfine splitting is 6 G. Varying the temperature from 135 to 4.2°K produced no change in these parameters. The splitting is not resolved at room temperature. As might be expected from inhomogeneous broadening considerations, the hyperfine interaction is unresolved on the fine structure components.

It is important to note that the hyperfine structure shown in Fig. 2 occurs for the central $\frac{1}{2} \rightarrow -\frac{1}{2}$ transition, i.e., the $g = 2$ line. This is in contrast to Wemple's

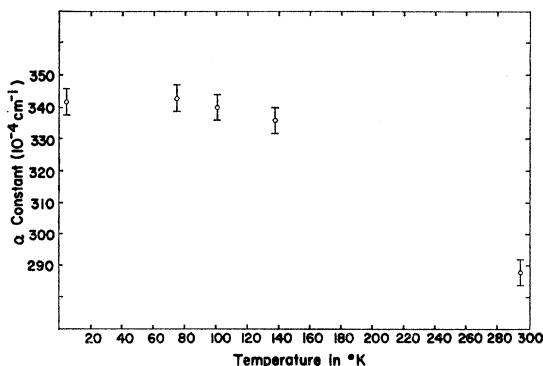


FIG. 3. The temperature dependence of the cubic field splitting constant a of Fe^{3+} on the Ta^{5+} site in KTaO_3 .

¹⁷ A. W. Hornig, R. C. Wemple, and H. E. Weaver, *J. Phys. Chem. Solids* **10**, 1 (1959).

¹⁸ K. A. Müller, *Helv. Phys. Acta* **31**, 173 (1958).

similar hyperfine structure which, surprisingly, occurs on a line with $g_{\text{eff}} = 4.24$. A line at $g \sim 4.28$ indicates strong axial plus rhombic crystal fields,^{19,20} a situation in which it is most unlikely for this hyperfine to be resolved. Wemple concluded that this line was due to Fe^{5+} ($3d^3$) in an axial field but such an assignment requires $g_{\text{eff}} \leq 4$. Thus, neither of these assignments is satisfactory for Wemple's hyperfine data.

The temperature dependence of the a constant for Fe^{3+} on the Ta^{5+} site is given in Fig. 3. We have not attempted to fit this temperature dependence to a phenomenological expression as done for Fe^{3+} and Gd^{3+} in SrTiO_3 .²¹ However, we can note that the temperature dependence of a for Fe^{3+} in KTaO_3 is greater than in SrTiO_3 between room temperature and about 100°K and that a for Fe^{3+} in KTaO_3 remains constant between 77 and 4.2°K, within experimental error.

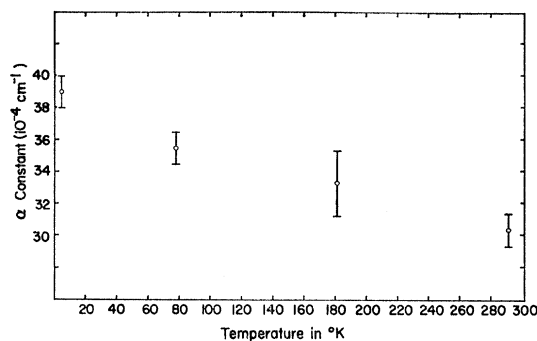


FIG. 4. The temperature dependence of the cubic field splitting constant a of Fe^{3+} on the K^{+1} site in KTaO_3 .

3. Fe^{3+} on the K^{+1} Site

In certain KTaO_3 samples, we have measured a cubic Fe^{3+} spectrum with different parameters from those given above. These parameters, $a = 30 \times 10^{-4} \text{ cm}^{-1}$ and linewidth $\Delta H = 15 \text{ G}$, indicate a quite different environment and this spectrum is assigned to Fe^{3+} on the other cubic site, the K^{+1} site. The very small a constant reflects the weak crystal field of this site.

The three samples which show this small a Fe^{3+} resonance all had titanium added to trap out free carriers as described in II. The surprising dividend of adding titanium is that we measure Fe^{3+} on the K^{+1} site rather than the Ta^{5+} site. In general, it appears that Fe^{3+} prefers the Ta^{5+} site in KTaO_3 , but some percentage does occupy the K^{+1} site. The data suggest that the titanium occupies the tantalum site and biases the Fe^{3+} site preference toward the K^{+1} site.

The temperature dependence of the a constant for Fe^{3+} on the K^{+1} site is given in Fig. 4. Here again, as in

¹⁹ T. Castner, Jr., G. S. Newell, W. C. Holton, and C. P. Slichter, *J. Chem. Phys.* **32**, 668 (1960).

²⁰ H. H. Wickman, M. P. Klein, and D. A. Shirley, *J. Chem. Phys.* **41**, 2113 (1965).

²¹ L. Rimai, T. Deutsch, and B. D. Silverman, *Phys. Rev.* **133A**, 1123 (1964).

the case for Fe^{3+} on the Ta^{5+} site, the uncertainty in the a value precludes curve fitting. We do note, however, that the 4.2°K value is greater than the 77°K value in contrast to the case for Fe^{3+} on the Ta^{5+} site.

4. Other Fe^{3+} Lines

Fe^{3+} lines characteristic of a strong axial field in the three $[100]$ directions ($S'_{\text{eff}} = \frac{1}{2}$, $g'_{\parallel} = 2$, $g'_{\perp} = 6$) are also seen in KTaO_3 for both sites. For Fe^{3+} at the Ta^{5+} site an adjacent oxygen vacancy is most likely responsible for the strong axial field but the source of a strong axial field for Fe^{3+} at the K^{+1} site is not evident.

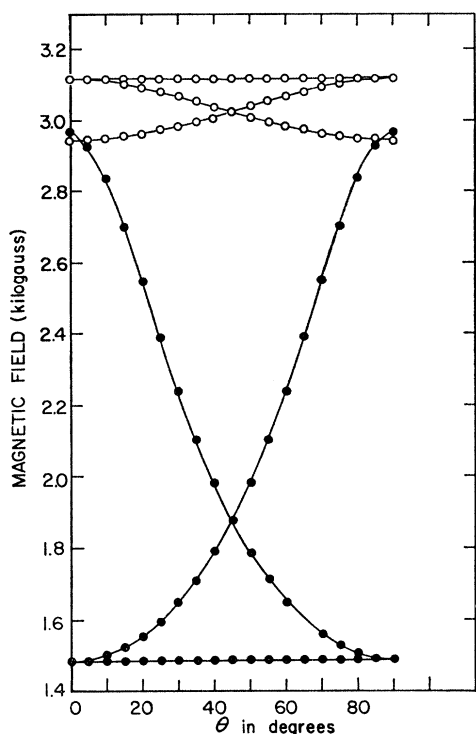


FIG. 5. Rotation spectrum for Ni^{3+} in KTaO_3 . The open circles are points for Ni^{3+} on the Ta^{5+} site called low-spin 1. Closed circles are points for Ni^{3+} on the K^{+1} site called high spin.

The site assignments for these axial lines is determined by the linewidths. We have not attempted to estimate D from the g shift as done for Fe^{3+} in SrTiO_3 .²² We also see a $g_{\text{eff}} = 4.27$ line characteristic of Fe^{3+} in a rhombic field.^{19,20}

C. Nickel Ion in KTaO_3

Nickel-doped KTaO_3 crystals show narrow (~ 10 G) EPR lines which have been assigned as arising from Ni^{3+} ions. At helium temperatures some broad EPR resonances were noted and assumed to be from divalent nickel. These broad lines were not investigated.

²² E. S. Kirkpatrick, K. A. Müller, and R. S. Rubins, Phys. Rev. **135**, A86 (1964).

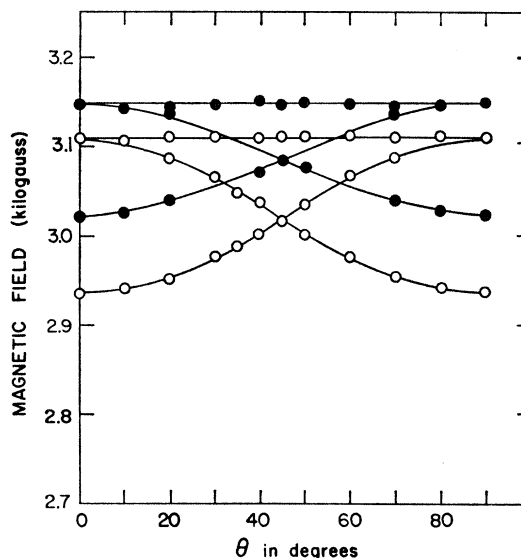


FIG. 6. Rotation spectrum for Ni^{3+} in $\text{K}_{1-x}\text{Na}_x\text{TaO}_3$ where $x \sim 0.3$. Open circles are points for Ni^{3+} on the Ta^{5+} site called low spin 1. Closed circles are points for Ni^{3+} on the Ta^{5+} site called low-spin 2.

Figure 5 gives the rotation spectrum for $\text{Ni}:\text{KTaO}_3$ and Fig. 6 gives the spectrum for $\text{Ni}:(\text{K}, \text{Na})\text{TaO}_3$ both taken at 77°K . These spectra show sets of three lines labeled high-spin and low-spin 1 and low-spin 2, each line reflecting axial symmetry along one of the $[100]$ crystal axes. The effective g values for these lines are given in Table I.

1. Low-Spin Ni^{3+}

The low-spin lines are attributed to Ni^{3+} at the octahedral Ta^{5+} site. The strong crystal field at this site stabilizes the low spin 2E state as the ground state with the 4T_1 state, the Hund's rule ground state, as the first excited state. See Fig. 7.

An axial field splits the 2E state into two Kramers doublets as in the familiar Cu^{2+} case. However, the g value formulas of the Cu^{2+} case, 1 hole, cannot be applied to low-spin Ni^{3+} , 3 holes, because the excited states of these two ions are quite different.

Lacroix *et al.*²³ have calculated the g value correction formulas for low-spin Ni^{3+} starting with triple products of single electron functions. Equations (3) are derived

TABLE I. Effective g values for Ni^{3+} in KTaO_3 .

Low-spin 1	Low-spin 2	High spin
$g_{\parallel} = 2.234 \pm 0.002$	$g_{\parallel} = 2.169 \pm 0.002$	$g_{\parallel} = 2.216 \pm 0.002$
$g_{\perp} = 2.111 \pm 0.002$	$g_{\perp} = 2.086 \pm 0.002$	$g_{\perp} = 4.423 \pm 0.008$

²³ R. Lacroix, U. Höchli, and K. A. Müller, Helv. Phys. Acta **37**, 627 (1964).

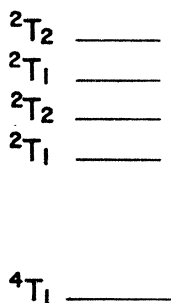
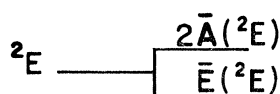


FIG. 7. Energy-level diagram for low-spin d^7 . Effect of axial crystal field shown on ground state only. Splittings are not to scale.



from their results and explicitly show how to take account of the near lying 4T_1 state.

$$\begin{aligned} g_{||}(V) &= 2 + (4\xi/\epsilon) + 2[\xi/E({}^4T_1)]^2, \\ g_{\perp}(V) &= 2 + (\xi/\epsilon) + 2[\xi/E({}^4T_1)]^2, \\ g_{||}(U) &= 2 + 2[\xi/E({}^4T_1)]^2, \\ g_{\perp}(U) &= 2 + (3\xi/\epsilon) + 2[\xi/E({}^4T_1)]^2. \end{aligned} \quad (3)$$

In Eqs. (3), U and V are the wave functions of the ground state 2E doublet, $E({}^4T_1)$ is the crystal-field splitting between the ground state 2E and the 4T_1 excited state, ξ is the spin-orbit coupling constant and ϵ is a function of the energy of the excited spin doublets as defined by Lacroix *et al.*²³

Since our low-spin g values have $g_{||} > g_{\perp}$, we solve the $g(V)$ equations eliminating ϵ and find an estimate of the splitting to the 4T_1 state. Table II gives $E({}^4T_1)$ arrived at in this manner and also an estimate of $10 Dq$ from the d^7 Tanabe and Sugano diagram. Values of $B = 660 \text{ cm}^{-1}$ and $\xi = 520 \text{ cm}^{-1}$ were used in the calculation.^{23,24}

$g_{||} > g_{\perp}$ indicates that the axial distortion is compressional for d^7 (opposite to d^9 case); therefore, we argue that the source of the distortion is a Jahn-Teller effect rather than an adjacent oxygen vacancy which would appear as an elongation of the octahedron. The assignment of a Jahn-Teller effect as the cause of the distortion is somewhat unsettling because we do not

TABLE II. Splitting of ${}^2E \rightarrow {}^4T_1$ and estimate of $10 Dq$ for low-spin Ni^{3+} in KTaO_3 .

Low-spin 1	Low-spin 2
$E({}^4T_1) = 2.8 \times 10^3 \text{ cm}^{-1}$	$E({}^4T_1) = 3.1 \times 10^3 \text{ cm}^{-1}$
$10Dq \approx 18 \times 10^3 \text{ cm}^{-1}$	$10Dq \approx 18.5 \times 10^3 \text{ cm}^{-1}$

²⁴ U. Höchli and K. A. Müller, Phys. Rev. Letters **12**, 730 (1964).

see a static to dynamic transition up to 330°K in contrast to other Ni^{3+} cases where this transition occurs at low temperatures.^{15,25-27}

In a number of crystals, the relaxation mechanism for low-spin Ni^{3+} has been assigned to an Orbach process²⁴ with the excited state of the split 2E cubic ground state, Fig. 7, as the Orbach process intermediate state. The increase in linewidth is written as $\Delta H \propto 1/T_1 = A e^{-\Delta/kT}$ where Δ is the $\bar{E}-2\bar{A}$ splitting and T_1 is the spin-lattice relaxation time. Figure 8 is a plot of ΔH , the increase in linewidth, versus $1/T$ for low-spin 1 Ni^{3+}

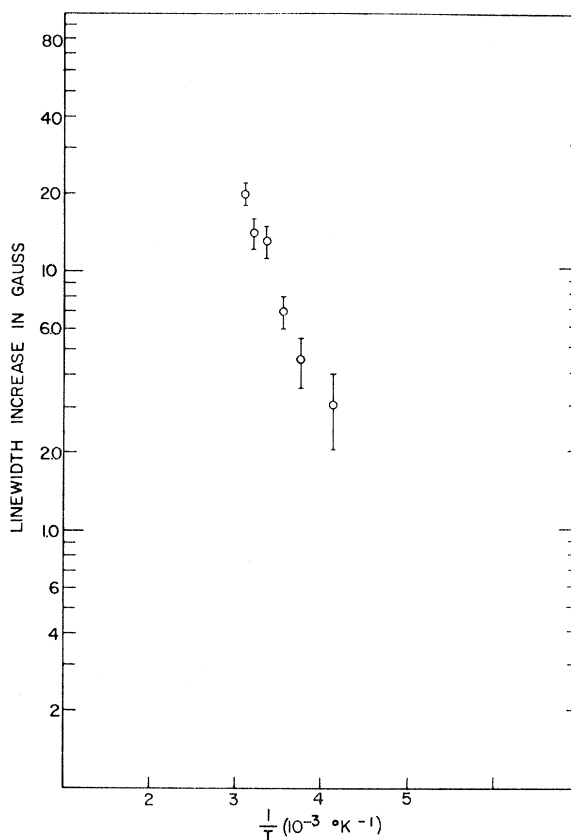


FIG. 8. Increase in line width versus $1/T$ for low-spin Ni^{3+} in KTaO_3 .

in KTaO_3 . If we assume that the relaxation is via an Orbach process, Fig. 8 yields a splitting Δ of $1400 \pm 150 \text{ cm}^{-1}$. This compares to 1530 ± 150 and 665 ± 50 for Ni^{3+} in Al_2O_3 and SrTiO_3 , respectively.²⁴

Extracting $10 Dq$ from the g formulas of Eqs. (3) and Δ from the line broadening should be viewed as conjectural because of broad assumptions contained in the calculations. In the $10 Dq$ calculation we have used the octahedral calculations of Lacroix *et al.*²³ thus

²⁵ S. Geschwind and J. P. Remeika, J. Appl. Phys. Suppl. **33**, 3705 (1962).

²⁶ U. Höchli, K. A. Müller, and P. Wyslign, Phys. Letters **15**, 5 (1965).

²⁷ W. Low and J. T. Suss, Phys. Letters **7**, 310 (1963).

ignoring axial splitting of the 4T_1 excited state. In the Δ calculation we have ignored other broadening mechanisms which might be present such as the onset of the static to dynamic Jahn-Teller behavior.

The second low-spin Ni^{3+} line occurs in crystals doped with Na. It is puzzling why placing Na^{+1} on the K^{+1} site leads to this new line rather than simple inhomogeneous broadening of the resonance. As shown in Fig. 1, these (K, Na) TaO_3 crystals undergo a ferroelectric phase transition. However, the Ni^{3+} resonance showed no change in the ferroelectric region presumably because the strong axial field already present above the Curie temperature masks the small lattice distortion occurring at the phase transition. In a somewhat similar case, Rubins and Low¹⁵ were able to measure the slight 110°K axial distortion of SrTiO_3 on Ni^{3+} ions which were already in a strong axial field caused by oxygen vacancies.

2. High-Spin Ni^{3+}

The three-line spectrum labeled high spin in Fig. 5 was recorded at 77°K. These lines broaden just above this temperature and are not seen above 150°K. The important aspect of this high spin line is that $g_{\perp}^{\text{eff}} = 2g_{\parallel}^{\text{eff}}$ within the experimental accuracy. Such a relation is familiar for d^3 configuration, e.g., Cr^{3+} , in an octahedral plus strong axial field. For d^7 , Ni^{3+} , to "look like" d^3 , we require a change of sign for the cubic field and, therefore, we assign the high-spin Ni^{3+} ion as substitutional near the K^{+1} site. Using the g shift formula $g = 2 - 8\lambda/10Dq$ and assuming a value of $\lambda \approx 200$ cm^{-1} we get an estimate of $10Dq$ of 7400 cm^{-1} . Notice the considerable change in crystal field between the K^{+1} site and the Ta^{5+} site, Table II, as seen by Ni^{3+} ion. Also, it is worth pointing out that Ni^{3+} on the K^{+1} site yields the sign of the crystal field whereas the Fe^{3+} on the K^{+1} site does not. Thus, for Ni^{3+} on the K^{+1} site the contribution of the 12 coordinated oxygen neighbors is greater than that of the eight coordinated tantalum ions, not a surprising result.

The source of the axial distortion for Ni^{3+} at the K^{+1} site is not evident. The ground state 4A_2 is not susceptible to a Jahn-Teller distortion and the type of charge compensation in this situation is unclear.

IV. DISCUSSION

As mentioned in the introduction, this work was undertaken in the hope of observing some effect upon the EPR parameters attributable to the ferroelectric nature of the host lattice. The two prototype experiments are the axial splitting of Fe^{3+} in BaTiO_3 at the ferroelectric transition¹⁷ and the $(T - T_c)^{-1}$ contribution to the cubic field splitting for Gd^{3+} in SrTiO_3 .²¹ The first experiment cannot be performed using KTaO_3 because it does not undergo a phase transition. Our attempts to see the effect of the (K, Na) TaO_3 phase

transition were unsuccessful but could probably be done with a rare-earth ion, e.g., Gd^{3+} , on the K^{+1} site. In this case the random site, the K^{+1} site itself, would be a third-neighbor site to the magnetic impurity and, hopefully, the Gd^{3+} fine structure would be resolved.

The second experiment was interpreted as an interaction between the effective +1 charge of Gd^{3+} on the Sr^{+2} site and Cochran's ferroelectric falling mode.^{8,21} It appears that the impurity must take advantage of the near cancellation of the cubic field at the Sr^{+2} or, in our case the K^{+1} site, Eq. 2, to demonstrate this behavior. Unoki and Sakudo²⁸ looked for the interaction with Gd^{3+} on the K^{+1} site in KTaO_3 and concluded that the interaction is absent and, furthermore, suggest it to be an anomaly of SrTiO_3 rather than to be expected in other perovskite ferroelectrics above the Curie temperature. They arrived at this conclusion because the cubic field splitting of Gd^{3+} , although increasing more than expected from thermal expansion between 77 and 4.2°K, does not have a term proportional to $(T - T_c)^{-1}$. Also, Fe^{3+} in BaTiO_3 does not show a $(T - T_c)^{-1}$ above the 120°C Curie temperature.

We reach a different conclusion on this point for two reasons. First, below about 60°K the dielectric constant and the falling mode frequency no longer follow the high temperature dependence so that a $(T - T_c)^{-1}$ dependence should not be expected. For example, no change is expected between 4.2 and 1.5°K because the falling mode has stopped falling. For Fe^{3+} in BaTiO_3 , the Fe^{3+} occupies the Ti^{4+} site and, therefore, does not utilize the near cancellation of Eq. 2. In this connection we note that Rimai *et al.*²¹ do indicate a $(T - T_c)^{-1}$ term for Fe^{3+} on the Ti site in SrTiO_3 but it is extremely small [total $(T - T_c)^{-1}$ change about 1 G].

The second reason has to do with our temperature results of Figs. 3 and 4. The cubic field splitting constant for Fe^{3+} on the Ta^{5+} site does not change, within experimental accuracy, between 77 and 4.2°K, whereas the constant for Fe^{3+} on the K^{+1} site does increase between 77 and 4.2°K. The inference we draw is that below 77°K the variation of the cubic field splitting due to thermal expansion has just about stopped,²⁹ thus the a constant for Fe^{3+} on the Ta^{5+} site is unchanged from 77 to 4.2°K. However, the Cochran falling mode changes frequency considerably between 77 and 4°K, although not proportional to $T - T_c$, and causes the increase of a for Fe^{3+} on the K^{+1} site.

ACKNOWLEDGMENTS

The author wishes to thank Professor R. V. Jones for his guidance and encouragement during this work. The author is grateful to W. R. Heller for helpful comments during the preparation of the manuscript.

²⁸ H. Unoki and T. Sakudo, J. Phys. Soc. Japan 21, 1730 (1966).

²⁹ W. M. Walsh, Jr., J. Jeener, and N. Bloembergen, Phys. Rev. 139, A1338 (1965).